



Cite this: *RSC Adv.*, 2025, 15, 37209

Received 11th July 2025  
Accepted 17th September 2025

DOI: 10.1039/d5ra04970a

rsc.li/rsc-advances

# LiCl-driven direct synthesis of mono-protected esters from long-chain dicarboxylic fatty acids

Yulong Kuang,<sup>a,b</sup> Xiaohui Yang,<sup>c</sup> Tianhong Qin,<sup>b</sup> Jigui Wang,<sup>b</sup> Paul Guo<sup>b</sup> and Chaozhe Jiang<sup>\*abd</sup>

A one-step mono-esterification method for long-chain dicarboxylic fatty acids [ $\text{HO}_2\text{C}(\text{CH}_2)_n\text{CO}_2\text{H}$ ;  $n \geq 14$ ] was developed using TFAA (trifluoroacetic anhydride) and LiCl as esterification reagents. This approach was particularly effective for synthesizing mono *tert*-butyl esters, which are key intermediates in the production of segments of semaglutide and tirzepatide—two blockbuster drugs with their 2024 sales valued in billions of dollars. The addition of LiCl critically enhanced the monoester selectivity over diester formation. Mechanistic studies suggest that this selectivity originates from a shielding effect, where LiCl interacts with one terminal carboxylic acid group.

## Introduction

Long-chain dicarboxylic fatty acids (LCDFAs) serve as critically important segments in drug molecules, facilitating specific electrostatic interactions between their terminal carboxylate anions and positively charged amino acid residues.<sup>1</sup> Semaglutide, the first LCDFA-containing therapeutic approved by the FDA (2017), incorporates octadecanedioic acid **1** (Fig. 1). Marketed as Ozempic®, Wegovy®, and Rybelsus®, it generated a cumulative sales of USD 27.98 billion in 2024.<sup>2</sup> Tirzepatide (approved in 2022/2023 as Mounjaro® and Zepbound®) features an extended carbon chain that enhances albumin binding,<sup>3</sup> and it achieved sales of USD 16.47 billion in 2024. As LCDFA-based therapeutics advance,<sup>4</sup> the highly selective synthesis of mono-protected LCDFAs improve the selectivity and reduce the costs during LCDFA segment incorporation.<sup>5</sup> However, the synthesis of mono-protected LCDFAs is still a persistent challenge.<sup>6</sup> To get these mono-protected LCDFAs, stoichiometric control of alcohols/activating reagents remains compromised by unavoidable diester formation.<sup>7</sup> Current methods predominantly rely on ring-opening of intramolecular anhydride intermediates with alcohols—effective for C5–C7 chains<sup>8</sup> but suffering from low yields in larger rings (Fig. 2a). Only few strategies directly achieve monoester selectivity over diesters by distinguishing the dicarboxylic acids using a heterogeneous strategy (Fig. 2b). Early heterogeneous

approaches adsorbed diacids [ $\text{HO}_2\text{C}(\text{CH}_2)_n\text{CO}_2\text{H}$ ;  $n = 3\text{--}8$  and 10] on alumina, followed by monomethyl esterification with diazomethane/dimethyl sulfate.<sup>9</sup> Phase-transfer catalysis enabled selective esterification of shorter diacids ( $n \leq 12$ ) with alkyl halides.<sup>10</sup> Ion-exchange resins catalyzed transesterification to mono alkyl esters ( $n \leq 12$ ).<sup>11</sup> Consequently, direct mono-selective synthesis, particularly of mono-*tert*-butyl esters from LCDFAs ( $n > 12$ ), remains an unmet challenge.

To address this challenge, we analyzed long-chain alkyl diacids as structures featuring two terminal hydrophilic carboxylic acid groups connected by a hydrophobic carbon backbone.<sup>12</sup> These carboxylic acid groups exhibited inherent affinity for metal cations *via* ionic or coordination bonding.<sup>13</sup>

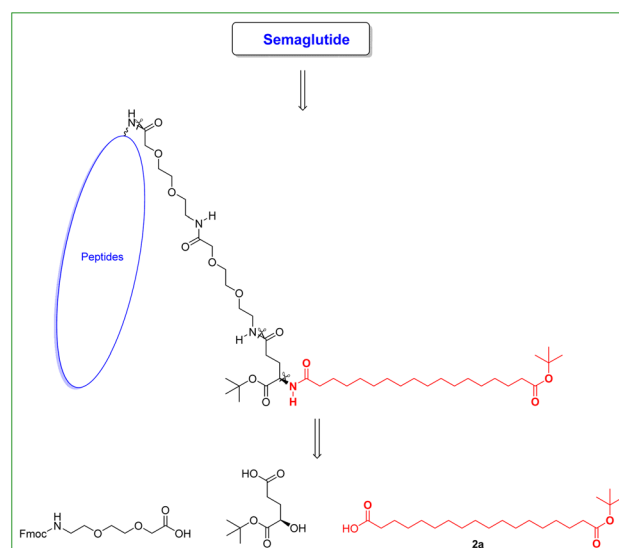


Fig. 1 Retrosynthetic analysis of the semaglutide's side chain and the key role of mono-*tert*-butyl ester.

<sup>a</sup>Southwest Jiaotong University, West Hightech Zone, Chengdu, Sichuan, 611756, People's Republic China. E-mail: kyl16320@163.com; jiangchaozhe@swjtu.edu.cn

<sup>b</sup>AstaTech (Chengdu) Biopharmaceutical Corporation, 488 Kelin West Road Wenjiang, Chengdu 611130, Sichuan, People's Republic China

<sup>c</sup>Suining Middle School, 96 Yucai Road, Suining, 629018, Sichuan, People's Republic China

<sup>d</sup>Engineering Research Center of Railway Industry of Operation Safety Assurance, National Railway Administration of P.R.C., Chengdu, Sichuan, 610031, China



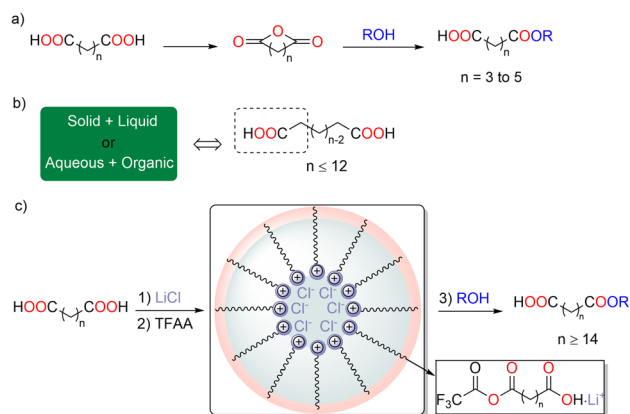


Fig. 2 Comparison of classic esterification methodologies and our strategy for constructing mono-protected esters. (a) Classical method by using the intramolecular anhydride intermediate; (b) other few successful strategies from heterogeneous system; (c) our strategy to differentiate the diacids.

Functionalization of one terminal carboxylate from a hydrophilic to a hydrophobic moiety maintained the inherent reverse micellar properties,<sup>14</sup> including the self-assembly competence and compartmentalization behaviour. Concurrently, intermolecular chain-chain interactions occurred between the hydrophobic segments<sup>15</sup> while partially shielding the metal-coordinated site, leaving a pre-activated esterification site (Fig. 2c). Building on classical esterification approaches,<sup>16</sup> we identified LiCl as a crucial reagent, achieving monoester: diester selectivity up to 50 : 1. Our strategy involved: (a) lithium

cation cluster formation with one carboxylic group through coordinative interactions; (b) exposure and activation of the distal carboxylic acid; and (c) selective mono-esterification even with excess reagents. A key observation confirmed this assembly behaviour: octadecanedioic acid **1** solubility in THF was significantly increased upon LiCl addition, yielding a clear mixture after the introduction of trifluoroacetic anhydride (TFAA) (Fig. S1). Conversely, reactions without LiCl produced cloudy suspensions.

## Results and discussion

Initial assessment confirmed TFAA's reactivity in diester formation from octadecanedioic acid **1**; reacting 2.4 equiv. *t*-BuOH with TFAA afforded diester **2a'** in 99% yield (Table 1, entry 13). Strikingly, introducing 1.0 equiv. LiCl reduced diacid conversion to 94% while achieving 7 : 1 mono/di selectivity (**2a** : **2a'**) (entry 12). Optimization revealed that 1.5 equiv. LiCl with 1.6 equiv. *t*-BuOH delivered dramatically improved selectivity (50 : 1, **2a** : **2a'**) and 79% isolated yield of monoester **2a** (entry 1). Other well-known Lewis acids were also evaluated based on the optimized conditions.<sup>17</sup> Among these, AlCl<sub>3</sub> afforded high conversion but generated multiple side products, and MgCl<sub>2</sub> provided marginal enhancement in monoester selectivity (entries 2 and 3). These data suggested that the Lewis acidity of LiCl might not be the major contributor in supporting mono-esterification. On the other hand, the influence of various lithium salts was investigated. Lithium bromide (LiBr) significantly suppressed the reactivity, resulting in a low monoester conversion. Lithium carbonate (Li<sub>2</sub>CO<sub>3</sub>) afforded the desired

Table 1 Optimization of reaction parameters<sup>a</sup>

Entry	Salt (equiv.)	<i>t</i> BuOH (equiv.)	Solvent	Time (h)	Yield <b>2a</b> <sup>b</sup>	<b>2a</b> : <b>2a'</b> <sup>c</sup>
1	LiCl (1.5 equiv.)	1.6	THF	24	79 (92)	50 : 1
2	AlCl <sub>3</sub> (1.5 equiv.)	1.6	THF	24	71 (84) <sup>d</sup>	35 : 1
3	MgCl <sub>2</sub> (1.5 equiv.)	1.6	THF	24	26 (84)	1 : 2
4	LiBr (1.5 equiv.)	1.6	THF	24	48 (82)	2 : 1
5	LiBr (1.5 equiv.)	1.6	THF	24	3 (4)	>99 : 1
6	Li <sub>2</sub> CO <sub>3</sub> (0.75 equiv.)	1.6	THF	24	78 (50)	3 : 1
7	LiOH · H <sub>2</sub> O (1.5 equiv.)	1.6	THF	24	Trace	
8	LiCl (1.5 equiv.)	1.6	MTBE	24	48 (55)	18 : 1
9	LiCl (1.5 equiv.)	1.6	2-Me-THF	24	Trace	
10	LiCl (1.5 equiv.)	1.6	DCM	24	ND	
11	LiCl (1.5 equiv.)	1.6	Toluene	24	ND	
12	LiCl (1.5 equiv.)	1.6	THF	24	11 (19)	>99 : 1
13	LiCl (1.0 equiv.)	2.4	THF	24	80 (94)	7 : 1
14	No LiCl	2.4	THF	24	>99 <sup>e</sup>	<1 : 99
15	LiCl (1.5 equiv.)	1.6	THF	48	73 (93)	18 : 1

<sup>a</sup> Experimental conditions: **1** (2 mmol), TFAA (4.8 mmol), *t*-BuOH (3.2 mmol), salts (3.0 mmol) in solvent (10 mL) at 25 °C for 24 h (entry 1); trace means only trace amount of product was detected; ND means no product was detected. <sup>b</sup> Isolated yield after column purification, data in parentheses indicate the conversion of compound **1**. <sup>c</sup> Selectivity of **2a** : **2a'** was determined *via* HPLC-ELSD. <sup>d</sup> The reported yield data corresponded to a 100-gram scale reaction. <sup>e</sup> The isolated yield is the product of **2a'**.



product, albeit in a moderate yield and a monoester-to-diester selectivity ratio of 3 : 1. In contrast, lithium hydroxide monohydrate ( $\text{LiOH} \cdot \text{H}_2\text{O}$ ) largely inhibited ester formation even though we fully dried the THF solution of  $\text{LiOH} \cdot \text{H}_2\text{O}$  and substrate **1** under high vacuum, followed by refilling of new anhydrous THF. These results established that the chloride anion is essential for selective monoester formation, which takes part in the key intermediate formation (entries 4–6). Studies on reaction robustness showed that elevated temperatures promoted THF-derived byproducts,<sup>18</sup> but alternative solvents compromised monoester yields (entries 7–10). However, extended reaction time (48 h) had negligible impact on the yield with decreased mono/di selectivity (entry 14 compared with entry 1, 18 : 1 to 50 : 1). Last but not the least, scale-up using 100 g of **1** under optimized conditions provided 71% isolated yield of **2a** without large selectivity compromise.

The optimized protocol was first evaluated with alternative alcohols (methanol, isopropanol, and benzyl alcohol), affording good-to-excellent monoester selectivity despite significantly reduced conversions. Steric analysis revealed enhanced selectivity with bulkier alcohols (mono/di ratio: **2a** > **4a** > **3a**; Fig. 3). Extension to diverse LCDFAs demonstrated broad substrate tolerance, delivering monoesters in moderate-to-good yields. Notably, the tirzepate intermediate **7a** was synthesized with 84% yield and 24 : 1 monoester/diester selectivity. The critical role of LiCl is evidenced by the predominant diester formation in its absence, even with stoichiometric alcohol, except for compounds **3a** and **5a**, which maintained monoester preference

despite reduced selectivity. Limitations were also observed: unsaturated analogs with internal alkenes (**8a**, **9a**; semaglutide/tirzepate precursors) required elevated temperatures due to low reactivity; shorter chain dioic acids (dodecanedioic acid **10**, malonic acid **11**, and 1,4-cyclohexanedicarboxylic acid **12**) yielded trace monoester; and terephthalic acid (**13**) showed no conversion under standard or harsher conditions.

To illustrate the role of LiCl in this methodology, control experiments were conducted. Upon the addition of LiCl ( $0.04 \text{ mg mL}^{-1}$ , 1.0 mM) to a solution of octadecanedioic acid **1** ( $0.2 \text{ mg mL}^{-1}$ , 0.75 mM), the characteristic transition exhibited a significant hyperchromic shift in the UV spectrum (Fig. 4a), with the  $\pi \rightarrow \pi^*$  transition occurring at  $\lambda = 212 \text{ nm}$  ( $\Delta\epsilon = 0.02 \text{ M}^{-1} \text{ cm}^{-1}$ ). This spectral modification demonstrated specific interactions between **1** and LiCl, consistent with the observed enhancement in solubility. Reversing the addition sequence from the standard protocol—introducing TFAA prior to LiCl—significantly reduced chemoselectivity (mono : di = 8 : 1 vs. 50 : 1; Fig. 4b). Nevertheless, this modified sequence still enabled monoester formation, suggesting that the LiCl would also interact with the bis(trifluoroacetyl) symmetrical anhydride intermediate **14** (structural formula:  $\text{CF}_3\text{C}(\text{O})\text{O}\text{C}(\text{O})\text{CH}_2\text{-(CH}_2\text{)}_{14}\text{CH}_2\text{C}(\text{O})\text{O}\text{C}(\text{O})\text{CF}_3$ ), facilitating its conversion to the corresponding monoester. The effect of LiCl was also evaluated; in particular, while a higher LiCl loading (>1.2 equiv.) improved the mono:di selectivity to >40 : 1, overstoichiometric amounts decreased the conversion (Fig. 4c). This inverse correlation further indicated that excess LiCl promotes

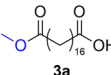
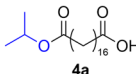
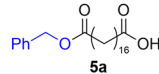
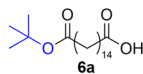
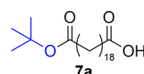
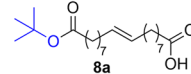
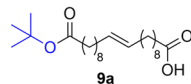
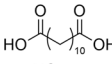
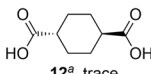
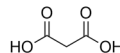
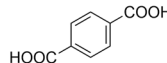
								
Condition	yield <b>3a</b>	<b>3a:3a'</b>	Condition	yield <b>4a</b>	<b>4a:4a'</b>	Condition	yield <b>5a</b>	<b>5a:5a'</b>
LiCl (1.5 equiv.), MeOH (1.6 equiv.)	45%	13:1	LiCl (1.5 equiv.), <i>i</i> PrOH (1.6 equiv.)	49%	22:1	LiCl (1.5 equiv.), BnOH (1.6 equiv.)	55%	21:1
LiCl (0 equiv.), MeOH (1.0 equiv.)	46%	3:1	LiCl (0 equiv.), <i>i</i> PrOH (1.0 equiv.)	28%	1:2	LiCl (0 equiv.), BnOH (1.0 equiv.)	52%	4:1
								
Condition	yield <b>6a</b>	<b>6a:6a'</b>	Condition	yield <b>7a</b>	<b>7a:7a'</b>	Condition <sup>a</sup>	yield <b>8a</b>	<b>8a:8a'</b>
LiCl (1.5 equiv.), <i>t</i> BuOH (1.6 equiv.)	58%	5:1	LiCl (1.5 equiv.), <i>t</i> BuOH (1.6 equiv.)	84%	24:1	LiCl (1.5 equiv.), <i>t</i> BuOH (1.6 equiv.)	47%	33:1
LiCl (0 equiv.), <i>t</i> BuOH (1.0 equiv.)	5%	1:4	LiCl (0 equiv.), <i>t</i> BuOH (1.0 equiv.)	22%	1:2	LiCl (0 equiv.), <i>t</i> BuOH (1.0 equiv.)	6%	1:3
								
Condition <sup>a</sup>	yield <b>9a</b>	<b>9a:9a'</b>						
LiCl (1.5 equiv.), <i>t</i> BuOH (1.6 equiv.)	46%	10:1	10 <sup>a</sup> , trace			12 <sup>a</sup> , trace		
LiCl (0 equiv.), <i>t</i> BuOH (1.0 equiv.)	22%	1:2	11 <sup>a</sup> , trace			13 <sup>a</sup> , NR		

Fig. 3 Substrate scope of alcohols and dioic acids. Reaction conditions: substrate (2 mmol), TFAA (4.8 mmol), alcohol (3.2 mmol), LiCl (3.0 mmol) in THF (10 mL) at 25 °C for 24 h. Yield of the pure monoester product isolated by column chromatography. Monoester/diester ratio was determined via HPLC-ELSD analysis. Trace means trace amount of product was detected via HPLC-ELSD. NR equals no reaction. <sup>a</sup>Reaction's temperature was 50 °C.



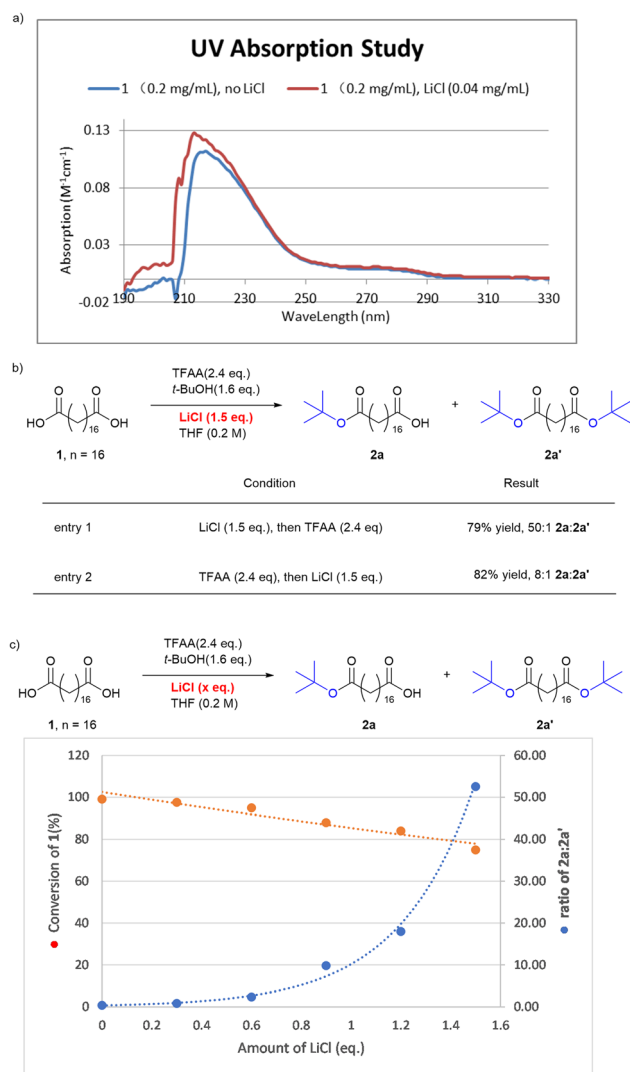


Fig. 4 Effect of LiCl on reactions. (a) UV absorption effect of LiCl in THF solution of compound 1; (b) the addition sequence effect of TFAA and LiCl; (c) the amount effect of LiCl on the selectivity 2a : 2a'.

decomposition of **14** to the unreactive carboxylic acid derivative, which failed to undergo esterification under these conditions.

To gain further insights,  $^1\text{H}$  NMR (THF- $d_8$ ) was performed, and it revealed an LiCl–**1** interaction, with a distinctive new signal ( $\delta$  2.83 ppm) at the  $\alpha$ -methylene group adjacent to the carbonyl group, emerging upon TFAA addition, which was distinct from those of **14** ( $\delta$  2.67 ppm) and free carboxylic acid **1** ( $\delta$  2.15 ppm) (Fig. 5a, S2 and S3 in SI).<sup>19</sup> The crude reaction mixture was characterized by ESI-MS, which detected the mono-activated species **15** (structural formula:  $\text{LiCl} \cdot \text{HO}-\text{CO}-\text{CH}_2-(\text{CH}_2)_{14}-\text{CH}_2-\text{CO}-\text{O}-\text{COCF}_3$ ) as  $[\text{TFA}-\mathbf{1} + \text{H}]^+$  (calcd  $m/z$  411.2, found 411.3) prior to alcohol addition (Fig. 5b), confirming single-carboxyl activation in the absence of the bis-activated intermediate **14**. On the other hand, complementary  $^{19}\text{F}$  NMR experiments in THF were carried out to monitor the reaction intermediates, given that all the activated species contained trifluoromethyl reporter groups. Fluorobenzene ( $\delta$  –114.0 ppm in THF) was used as an internal reference.

Commercial reagents were first characterized: trifluoroacetic anhydride (TFAA,  $\delta$  –76.3 ppm), trifluoroacetic acid (TFAH,  $\delta$  –76.7 ppm), and methyl trifluoroacetate ( $\delta$  –75.9 ppm) (Fig. S4–S6 in SI). Next, a mixture of TFAA (2.4 mmol) and LiCl (1.5 mmol) in THF (5 mL) was analyzed (Fig. 5c). After stirring for 30 min,  $^{19}\text{F}$  NMR revealed a near-complete consumption of TFAA ( $\delta$  –76.3 ppm) and a dominant new peak at  $\delta$  –76.7 ppm. This species was observed for a prolonged reaction time (up to 3 hours). To identify the intermediate, methanol (5 equiv.) was added as a trapping agent, yielding methyl trifluoroacetate ( $\delta$  –75.9 ppm) as an exclusive product. These observations confirmed that LiCl promoted TFAA disproportionation:  $\text{CF}_3\text{C}(\text{O})-\text{O}-\text{C}(\text{O})\text{CF}_3 + \text{LiCl} \rightarrow \text{CF}_3\text{COOLi} + \text{CF}_3\text{COCl}$ .<sup>20</sup> The resulting lithium trifluoroacetate ( $\text{CF}_3\text{COOLi}$ ) and trifluoroacetyl chloride ( $\text{CF}_3\text{COCl}$ ) displayed coincident  $^{19}\text{F}$  NMR resonances near  $\delta$  –76.6 ppm (Fig. 5c), overlapping with the signal of trifluoroacetic acid ( $\delta$  –76.7 ppm) and appearing as a single combined peak. Under these optimized conditions,  $^{19}\text{F}$  NMR analysis revealed a single coalesced signal at  $\delta$  –76.6 ppm (Fig. 5d) following TFAA addition (0.5 h), which was distinct from the free TFAA ( $\delta$  –76.3 ppm) and identical to the characteristic shift observed in the TFAA/LiCl pre-mixing system (Fig. 5c). This signal remained unchanged after extended stirring (3 h). Subsequent methanol addition (10 mmol, 5 equiv.) also yielded methyl trifluoroacetate (4.0% from all  $^{19}\text{F}$  integrations;  $\delta$  –75.9 ppm) within 1 h, and with prolonged stirring, (18 h) the concentration increased to 27.2%. Combined with results for product **3a**, the signal at  $\delta$  –76.6 ppm was assigned to overlapping resonances from both **15** and trifluoroacetyl chloride—the latter was identified as the key byproduct under these conditions.

To check the effect of addition sequence of LiCl,  $^1\text{H}$  NMR (THF- $d_8$ ) spectra were evaluated, which supported that the addition of LiCl to **14** could induce disproportionation ( $\delta$  2.67 to 2.83 ppm; Fig. S2, from spectrum E to spectrum F), giving the same mono-activated species **15**. In  $^{19}\text{F}$  NMR studies, upon addition of TFAA to a THF solution of **1**, two distinct  $^{19}\text{F}$  signals around  $\delta$  –76.7 ppm emerged (Fig. 5e) in the absence of residual TFAA. The downfield signal was unequivocally assigned to **14**. Subsequent introduction of LiCl induced complete signal conversion to a single peak ( $\delta$  –76.6 ppm), identical to the spectrum obtained when LiCl was pre-mixed with TFAA (Fig. 5c). Crucially, methanol quenching experiments also yielded methyl trifluoroacetate ( $\delta$  –75.9 ppm). This confirmed the capacity of LiCl to react with intermediate **14**, which was consistent with salt metathesis,  $\text{R}-\text{C}(\text{O})\text{O}-\text{C}(\text{O})\text{CF}_3 + \text{LiCl} \rightarrow \text{R}-\text{COOLi} + \text{CF}_3\text{COCl}$ , generating trifluoroacetyl chloride and mono-activated species **15**. In parallel, the reaction of dodecanedioic acid **10**—which yielded only a trace amount of mono-*tert*-butyl ester—was monitored by  $^1\text{H}$  NMR (THF- $d_8$ ) under optimized conditions (Fig. 5f). Only a minor fraction of compound **10** was converted into a new species, characterized by a resonance at  $\delta$  2.83 ppm in the  $^1\text{H}$  NMR spectrum, while the majority of the substrate remained unreacted. Crucially, no signal corresponding to a trifluoroacetyl mixed anhydride intermediate (such as structure **14**, which displayed a characteristic signal at  $\delta$  2.67 ppm) was observed. These results





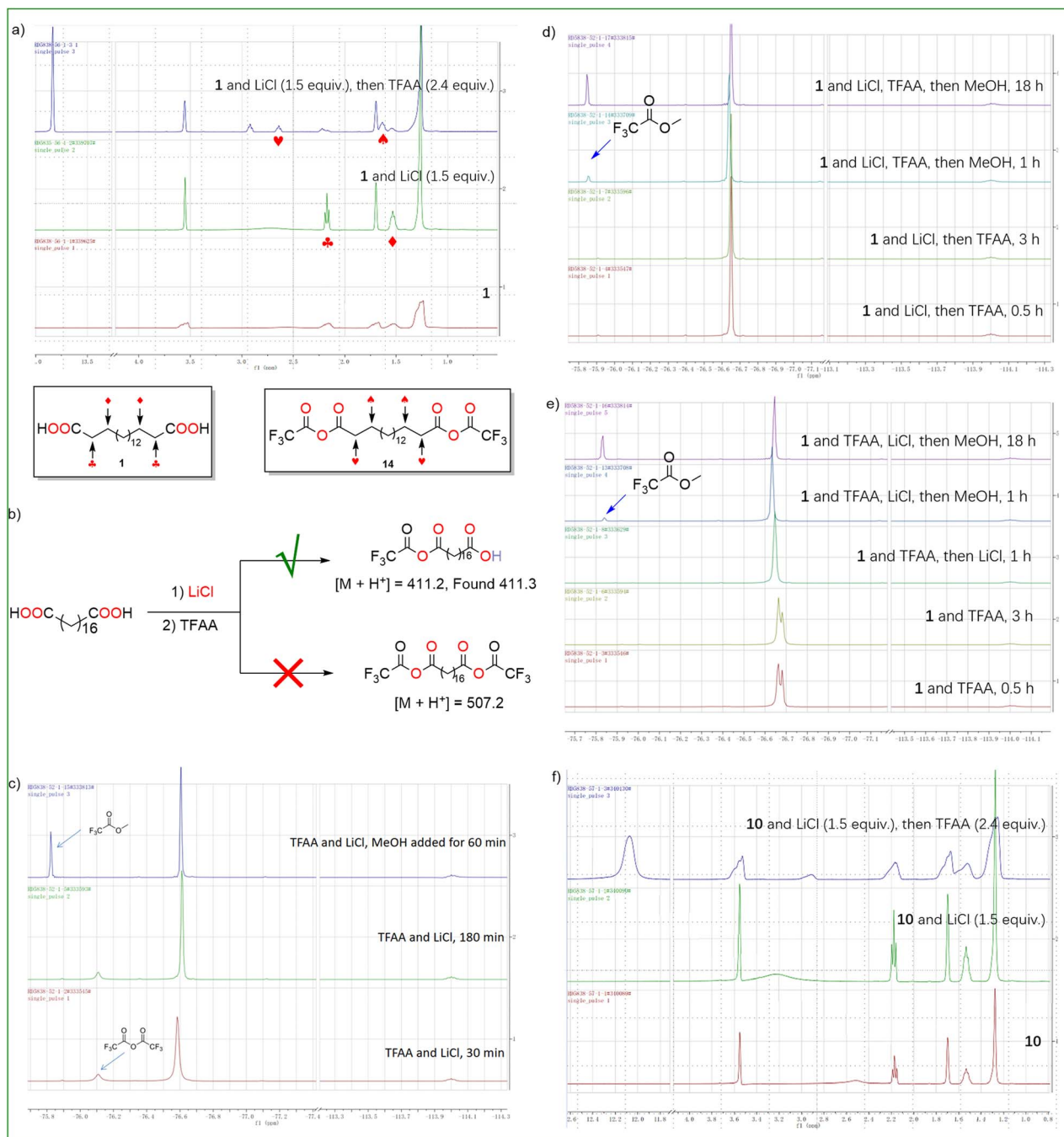


Fig. 5 Spectroscopic mechanistic studies (NMR/MS), and reactivity comparison with inactive substrate. (a)  $^1\text{H}$  NMR studies of reaction process for active substrate **1**; (b) ESI-MS experiment for mono-activation intermediate; (c)  $^{19}\text{F}$  NMR studies for LiCl effect on TFAA in THF; (d)  $^{19}\text{F}$  NMR studies for active substrate **1**; (e)  $^{19}\text{F}$  NMR studies for adding the TFAA prior to LiCl; (f)  $^1\text{H}$  NMR studies for inactive substrate **10** under the optimized condition.

indicated that shorter-chain dicarboxylic acids ( $n \leq 10$ ) were unable to form the supramolecular assembly required to effectively sequester the chloride anion. Consequently, this inability led to an uncontrolled degradation of TFAA in the presence of LiCl, thereby inhibiting the ester formation.

Collectively, these studies demonstrated that LiCl promoted trifluoroacetyl mixed anhydride and TFAA decomposition *via* nucleophilic attack at the trifluoroacetyl moiety, forming the

required intermediates and trifluoroacetyl chloride. This pathway aligned well with the experimental observations, wherein LiCl (i) reduced the reaction conversion (Fig. 4c) and (ii) completely suppressed the esterification of short-chain fatty diacids (C3–C12, Fig. 3). For long-chain dicarboxylic acids ( $n \geq 14$ ), hydrophobic encapsulation and steric shielding attenuated chloride's nucleophilic accessibility, significantly reducing the

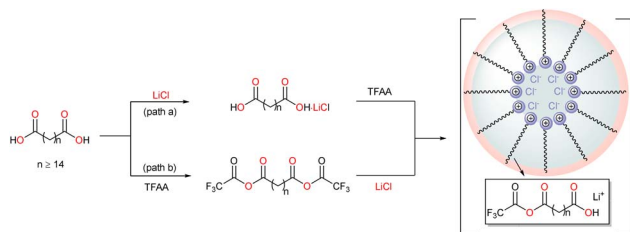


Fig. 6 Mechanistic pathways to the key mono-esterification intermediate.

decomposition pathways while maintaining the catalytic cyclization efficacy.

The following mechanistic proposal highlighting the role of LiCl was given: (a)  $\text{Li}^+$  coordinates with one carboxylic acid; (b) hydrophobic chain packing partially exposes the distal carboxylic acid and hides the chloride; (c) the exposed site undergoes selective mono(trifluoroacetyl) mixed anhydride formation; and the (d) corresponding alcohol reacts with the mono-(trifluoroacetyl) mixed anhydride to complete the mono-esterification of diacids (Fig. 6, path a). When a symmetrical bis(trifluoroacetyl) mixed anhydride intermediate is preformed, the LiCl in the system would attack the more electron deficient trifluoroacetyl group to disproportionate the bis(trifluoroacetyl) mixed anhydrides to mono-activated assemblies (Fig. 6, path b).

## Conclusions

In summary, we developed a highly selective mono-esterification protocol for long-chain dicarboxylic fatty acids (LCDFAs;  $n \geq 14$ ), achieving unprecedented mono-/di-ester selectivity (up to 50 : 1). This method demonstrated excellent functional group tolerance across LCDFA substrates, with 100-gram scale synthesis confirming its industrial viability. Mechanistic studies established that the LiCl-mediated mono-carboxylate activation and selective mono(trifluoroacetyl) mixed anhydride formation drive the observed selectivity. This methodology enables large-scale production of key peptide therapeutic intermediates.

## Author contributions

Y. Kuang and T. Qin discovered and developed the reaction. Y. Kuang, T. Qin and J. Wang performed the experiments. Y. Kuang, X. Yang, P. Guo and C. Jiang conceived and designed the investigation. Y. Kuang and C. Jiang wrote the manuscript.

## Conflicts of interest

The authors declare no conflict of interest.

## Data availability

Experimental procedures, characterization data and NMR spectra of the new compounds are included in the

supplementary information (SI). Supplementary information is available. See DOI: <https://doi.org/10.1039/d5ra04970a>.

## Acknowledgements

We appreciate Southwest Jiaotong University (Grant No. R113622H01064) and AstaTech (Chengdu) Biopharmaceutical Corporation for experimental and financial support. We also thank the AstaTech (Chengdu) Biopharmaceutical Corporation's Analytical & Testing Center for NMR and MS analysis.

## Notes and references

- 1 C. E. Callmann, C. L. M. LeGuyader, S. T. Burton, M. P. Thompson, R. Hennis, C. Barback, N. M. Henriksen, W. C. Chan, M. J. Jaremko, J. Yang, A. Garcia, M. D. Burkart, M. K. Gilson, J. D. Momper, P. A. Bertin and N. C. Gianneschi, *J. Am. Chem. Soc.*, 2019, **141**, 11765.
- 2 N. A. McGrath, M. Brichacek and J. T. Njardarson, *J. Chem. Educ.*, 2010, **87**, 1348.
- 3 J. Lau, P. Bloch, L. Schäffer, I. Pettersson, J. Spetzler, J. Kofoed, K. Madsen, L. B. Knudsen, J. McGuire, D. B. Steensgaard, H. M. Strauss, D. X. Gram, S. M. Knudsen, F. S. Nielsen, P. Thygesen, S. Reedt-Runge and T. Kruse, *J. Med. Chem.*, 2015, **58**, 7370.
- 4 A. A. Bhattacharya, T. Grüne and S. Curry, *J. Mol. Biol.*, 2000, **303**, 721.
- 5 (a) N. S. Curvey, S. E. Luderer, J. K. Walker and G. W. Gokel, *Synthesis*, 2014, **46**, 2771; (b) X. Liu, N. Zhang, X. Gu, Y. Qin, D. Song, L. Zhang and S. Ma, *ACS Comb. Sci.*, 2020, **22**, 821; (c) M. O. Frederick, R. A. Boyse, T. M. Braden, J. R. Calvin, B. M. Campbell, S. M. Changi, S. R. Coffin, C. Condon, O. Gowran, J. M. Groh, S. R. Groskreutz, Z. D. Harms, A. A. Humenik, N. J. Kallman, N. D. Klitzing, M. E. Kopach, J. K. Kretsinger, G. R. Lambertus, J. T. Lampert, L. M. Maguire, H. A. Moynihan, N. S. Mullane, J. D. Murphy, M. E. O'Mahony, R. N. Richey, K. D. Seibert, R. D. Spencer, M. A. Strega, N. Tandogan, F. L. Torres Torres, S. V. Tsukanov and H. Xia, *Org. Process Res. Dev.*, 2021, **25**, 1628.
- 6 (a) X. X. Zhang, C. A. H. Prata, J. A. Berlin, T. J. McIntosh, P. Barthelemy and M. W. Grinstaff, *Bioconjugate Chem.*, 2011, **22**, 690; (b) V. Santacroce, F. Bigi, A. Casnati, R. Maggi, L. Storaro, E. Moretti, L. Vaccaro and G. Maestri, *Green Chem.*, 2016, **18**, 5764.
- 7 N. Jain, Y. Arntz, V. Goldschmidt, G. Duportail, Y. Mély and A. S. Klymchenko, *Bioconjugate Chem.*, 2010, **21**, 2110.
- 8 Selected examples: (a) J. Poldy, R. Peakall and R. A. Barrow, *Tetrahedron Lett.*, 2008, **49**, 2446; (b) R. Geyer, U. Nordemann, A. Strasser, H. Wittmann and A. Buschauer, *J. Med. Chem.*, 2016, **59**, 3452; (c) C. Beato, C. Pecchini, C. Cocconcelli, B. Campanini, M. Marchetti, M. Pieroni, A. Mozzarelli and G. Costantino, *J. Enzyme Inhib. Med. Chem.*, 2016, **31**, 645; (d) Y. Gao, M. J. Haren, E. E. Moret, J. J. M. Rood, D. Sartini, A. Salvucci, M. Emanuelli, P. Craveur, N. Babault, J. Jin and N. I. Martin, *J. Med. Chem.*, 2019, **62**, 6597.



- 9 H. Ogawa, T. Chihara and K. Taya, *J. Am. Chem. Soc.*, 1985, **107**, 1365.
- 10 J. D. L. Zerda, G. Barak and Y. Sasson, *Tetrahedron*, 1989, **45**, 1533.
- 11 M. Saitoh, S. Fujisaki, Y. Ishii and T. Nishiguchi, *Tetrahedron Lett.*, 1996, **37**, 6733.
- 12 F. R. Taylor, D. Wen, E. A. Garber, A. N. Carmillo, D. P. Baker, R. M. Arduini, K. P. Williams, P. H. Weinreb, P. Rayhorn, X. Hronowski, A. Whitty, E. S. Day, A. Boriack-Sjodin, R. I. Shapiro, A. Galdes and R. Blake Pepinsky, *Biochemistry*, 2001, **40**, 4359.
- 13 (a) G. Murdachaew, M. Valiev, S. M. Kathmann and X. Wang, *J. Phys. Chem. A*, 2012, **116**, 2055; (b) A. Sthoer, J. Hladílková, M. Lund and E. Tyrode, *Phys. Chem. Chem. Phys.*, 2019, **21**, 11329.
- 14 N. M. Correa, J. J. Silber, R. E. Riter and N. E. Levinger, *Chem. Rev.*, 2012, **112**, 4569.
- 15 P. B. Miranda, V. Pflumio, H. Saijo and Y. R. Shen, *J. Am. Chem. Soc.*, 1998, **120**, 12092.
- 16 (a) M. Stacey, E. J. Bourne, J. C. Tatlow and J. M. Tedder, *Nature*, 1949, **164**, 705; (b) A. K. Chakraborti and R. Gulhane, *Tetrahedron Lett.*, 2003, **44**, 6749.
- 17 The LiCl was also widely used as Lewis acid, selected examples: (a) S. Bera, R. C. Samanta, C. G. Daniliuc and A. Studer, *Angew. Chem., Int. Ed.*, 2014, **53**, 9622; (b) M. V. Marques and M. M. Sá, *J. Org. Chem.*, 2014, **79**, 4650; (c) Y. Reddi and R. B. Sunoj, *ACS Catal.*, 2017, **7**, 530.
- 18 M. Y. Bhat, A. H. Padder, R. Gupta and Q. N. Ahmed, *J. Org. Chem.*, 2023, **88**, 14323.
- 19 For more information, see SI.
- 20 Selected similar examples: (a) J. Heliński, Z. Skrzypczyński, J. Wasiak and J. Michalski, *Phosphorus, Sulfur, Silicon Relat. Elem.*, 1990, **54**, 225; (b) O. V. Kupriyanova, V. A. Shevyrin, Y. M. Shafran, A. T. Lebedev, V. A. Milyukov and V. L. Rusinov, *Drug Test. Anal.*, 2020, **12**, 1154; (c) A. F. C. Flores, P. F. Rosales, J. L. Malavolta and D. C. Flores, *J. Braz. Chem. Soc.*, 2024, **25**, 1439.

